THE JOURNAL OF PHYSICAL CHEMISTRY B LETTERS

2005, *109,* 18719−18722
Published on Web 09/16/2005

Preparation of Large-Pore Mesoporous Nanocrystalline TiO_2 Thin Films with Tailored Pore Diameters

Kesong Liu,[†,§] Honggang Fu,[*,†] Keying Shi,[†] Fengshou Xiao,[‡] Liqiang Jing,[†] and Baifu Xin[†]

Laboratory of Physical Chemistry, School of Chemistry and Materials Science, Heilongjiang University, 150080 Harbin P. R. China, Department of Chemistry & State Key Laboratory of Inorganic Synthesis and Preparative Chemistry, Jilin University, 130012 Changchun P. R. China, School of Chemical Engineering, Harbin Engineering University, 150001 Harbin P. R. China

Received: August 12, 2005; In Final Form: September 3, 2005

A novel and facile synthesis route to large-pore mesoporous nanocrystalline anatase thin films with tunable pore diameters in narrow distribution of sizes ranging from 8.3 to 14 nm is reported, using triblock copolymer as the template and $Ti(OBu^n)_4$ as the inorganic precursor. The obtained materials were characterized by X-ray diffraction, scanning electron microscopy, transmission electron microscopy, and nitrogen adsorption. A reasonable formation mechanism is also presented in this work.

1. Introduction

Recently, mesostructured materials with large pore sizes have attracted much attention because of their potential applications in large molecule separation, catalysis, medical implants, and shape-selective heterojunctions.[1−4] By using the amphiphilic triblock copolymer $HO(CH_2CH_2O)_{20}(CH_2CH(CH_3)O)_{70}(CH_2CH_2O)_{20}H$ (Pluronic P123) as the structure-directing agent, silica-based mesostructured materials with large pore sizes of 8.5−30 nm have been successfully synthesized.[5−8] In comparison to mesoporous silica materials, mesoporous nanocrystalline anatase (meso-nc-TiO_2) thin film materials with large pores have more interesting applications, associated to their characteristic optic, electronic, and magnetic properties.[9,10] However, little work has been reported about meso-nc-TiO_2 thin film materials with the pore size up to 8 nm using P123 as template.[11−15] This makes it difficult to infiltrate the heterogeneous components into the pores efficiently. For example, polymers suffer a loss of conformational entropy when they are confined in pores whose radii are less than their radii of gyration. So, to maximize the utility of mesoporous TiO_2 materials, it is essential to synthesize large-pore meso-nc-TiO_2. It has been reported in the literature[16] that, in the P123−alcohol−water system, the *n*-alkyl alcohol (BuOH) will solubilize the hydrophobic−hydrophilic interface of the micelle, thus swelling the micelle. The degree of swelling is proportional to the amount of added alcohol. Butanol acts as a swelling agent or cosurfactant in block copolymer−water systems. Unlike nonpolar oils, the polar −OH headgroup of BuOH is believed to be located at the hydrophilic−hydrophobic interface between PEO and PPO blocks to help in stabilizing the liquid crystals and determining their interfacial curvatures.[6,16−20] Since the mesopore size is, to a large extent, determined by the effective volume of the hydrophobic core of surfactant arrays, we think using butanol as the cosurfactant will open up the possibility of synthesizing large-pore mesoporous TiO_2 materials. Ozin and co-workers have reported the synthesis of 2-D hexagonal meso-nc-TiO_2 using P123 as the template, $Ti(OEt)_4$ as the inorganic precursor, and *n*-butanol as the solvent, but the pore size of their obtained mesoporous materials is only 7.3 nm.[15] This can be attributed to the fact that the mesopore diameter partly depends on the nature of the alkoxide groups of the inorganic precursors.[21]

On the basis of the above facts, an idea is proposed by us, focused on the preparation of large-pore meso-nc-TiO_2 thin films by using a unique titanium alkoxide as the inorganic source. We think $Ti(OBu^n)_4$ is a particularly interesting candidate that possesses the following two paramount advantages: (1) butanol released in situ and (2) its linearity and larger dimensions compared with those of $Ti(OBu^t)_4$, $Ti(OPr^i)_4$, or $Ti(OEt)_4$. Both unique advantages facilitate the synthesis of large-pore meso-nc-TiO_2 thin films in a $Ti(OBu^n)_4$−P123−EtOH−HCl system using a one-step synthesis strategy through the well-documented evaporation-induced self-assembly (EISA) approach. Furthermore, by adjusting the amount of $Ti(OBu^n)_4$, thus the amount of BuOH released in situ, while other synthesis parameters kept constant, we are able to easily tailor the mesopore size in a wide range that has not been achieved in such way in a titanium-based system previously.

Here, we will focus on describing the synthesis and characterization of transparent meso-nc-TiO_2 thin films with uniform large pore size of 10.2 nm (designated HLJU-10). A meso-nc-TiO_2 thin film with pore size of about 10 nm is the optimal structure for photovoltaics, which is the exciton diffusion length of titania.[9] Such novel materials present a good host porous structure to form a novel heterojunction through growth of a variety of wide band-gap semiconductors and assembling functional polymers, noble metals, carbon nanotubes, and other components in the large mesopore channels, which could be

* Tel.: 86-0451-86608458. Fax: 86-0451-86673647. E-mail: fuhg@vip.sina.com.
† Heilongjiang University.
‡ Jilin University.
§ Harbin Engineering University.

10.1021/jp054546p CCC: $30.25

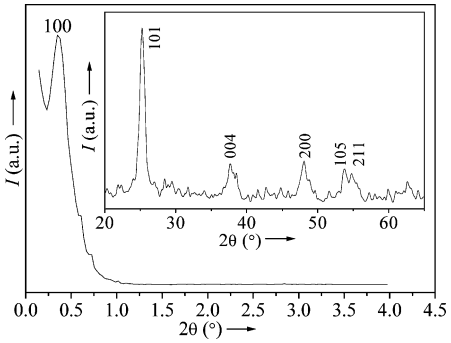

Figure 1. SAXRD and WAXRD (inset) patterns of calcined mesoporous HLJU-10 prepared using P123 as template and $(Ti(OBu^n)_4)$ as inorganic precursor. I = intensity (arbitrary units). SAXRD and WAXRD patterns were obtained on a Siemens D5005 diffractometer and a Rigaku D/max-IIIB diffractometer with Cu Kα radiation, respectively.

useful for the development of improved efficiency in solar cells, battery electrodes, sensors, and (photo)catalytic applications, and thus designing novel functionalized mesostructured materials possessing additional physical and chemical properties.

2. Experimental Section

Typical Synthesis of HLJU-10. The initial solution is made by slowly adding EtOH/P123 (MW = 5800, Aldrich) solution to the mixture of $Ti(OBu^n)_4$/HCl. The weights in grams of each component are $Ti(OBu^n)_4$/EtOH/HCl/P123 = 2.7 g/12 g/3.2 g/1 g. The resulting sol was then aged at room temperature, and uniform and transparent thin films were produced by dip-coating the indium−tin oxide (ITO)-coated glass substrates at a constant withdrawal rate of 1 mm/s. After aging the films at room temperature and 50−60% relative humidity (RH) for 24 h, the as-synthesized thin films were then calcined at 350 °C (ramp of 1 °C min^{-1}) for 4 h in air.

3. Results and Discussion

Small-angle and wide-angle X-ray diffraction (SAXRD and WAXRD) patterns of calcined HLJU-10 are shown in Figure 1. The SAXRD pattern clearly shows a main peak at 0.33°, which indicates d_{100} (26.7 nm) of mesoporous structure (Figure 1). Because there is a shoulder peak at around 0.4−0.6°, a long-range ordered mesostructure is expected, because a strong first peak and a weak second peak are generally found in ordered mesostructures.[14] Although the SAXRD pattern was suggestive of hexagonally ordered or at least ordered mesoporous structure, the scanning electron microscope (SEM) and transmission electron microscopy (TEM) observations revealed short-range ordered mesoporous structure. Therefore, it is considered that a small amount of ordered mesostructures are included in the calcined HLJU-10 sample. The WAXRD pattern of the calcined HLJU-10 is shown in the inset of Figure 1. It clearly shows the presence of nanocrystalline anatase in the calcined sample, because five crystal peaks can be observed and indexed as (101), (004), (200), (105), and (211), respectively. The crystallite size calculated from the Scherrer equation using the (101) diffraction peak of anatase is about 8.5 nm. High-resolution transmission electron microscopy (HRTEM) (Figure 2B) observation further substantiated WAXRD results showing the presence of anatase phase in the calcined sample with about 8 nm of crystallite size.

Representative TEM image of mesoporous HLJU-10 after calcination shown in Figure 2A exhibits a two-dimensional hexagonal structure, which possesses mesopores of 10 nm in diameter. Figure 2B shows an HRTEM image of nc-TiO_2. The lattice fringes corresponding to (101) (d_{101} = 0.352 nm) crystallographic planes of anatase are most frequently observed in the calcined sample, which is the typically observed surface for naturally occurring anatase. The TEM observation is consistent with the XRD results.

Typical SEM images of calcined HLJU-10 are shown in Figure 3. One can clearly see that the pores in calcined HLJU-10 are quasi-hexagonal in shape and the mesopores (around 10 nm) are very uniform. The presence of highly uniform mesopores in the films is desirable for the efficient dissociation of excitons. In this overall view of the mesopores, although no long-range order is apparent, some small organized domains can be observed. N_2 sorption analysis further corroborates SEM and TEM observations showing the presence of large mesopores in calcined HLJU-10 (see below). Similar results can be observed in other areas.

The N_2 adsorption−desorption isotherm (Figure 4) obtained for calcined HLJU-10 shows a type IV curve with a sharp capillary condensation step at higher relative pressure compared with other reports,[13−15] and this implies that the calcined sample

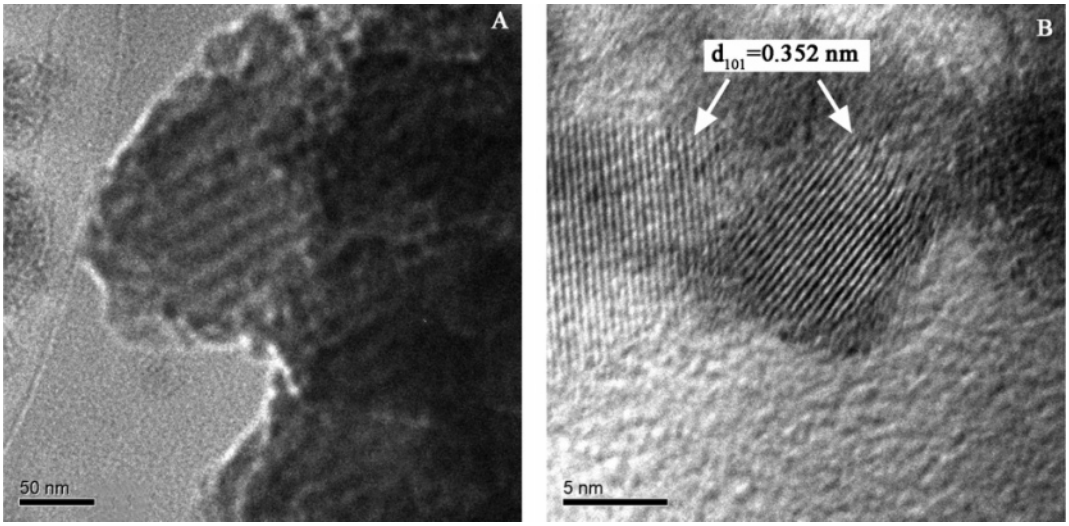

Figure 2. Typical TEM micrographs at two different magnifications of mesoporous HLJU-10 calcined at 350 °C for 4 h. (A) TEM micrograph of calcined mesoporous HLJU-10 which exhibits short-range ordered mesostructure. (B) HRTEM micrograph of nc-TiO_2 particles which clearly exhibits (101) faces. TEM experiment was performed on a JEM-3010 electron microscope (JEOL, Japan) with an acceleration voltage of 300 kV.

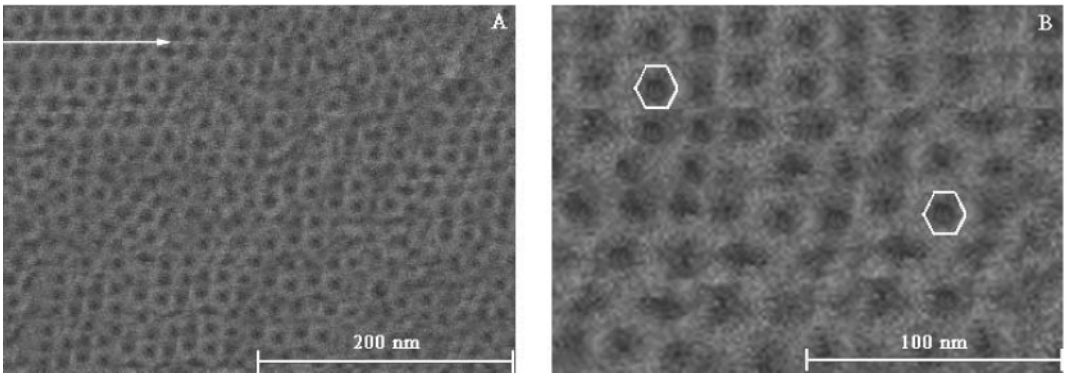

Figure 3. Representative SEM images of calcined mesoporous HLJU-10 at two different magnifications: (A) Lower-magnification SEM image shows short-range ordered mesostructure; (B) higher-magnification SEM image shows quasi-hexagonal mesopores. The SEM micrographs were taken using a Philips XL-30-ESEM-FEG instrument operating at 20 kV.

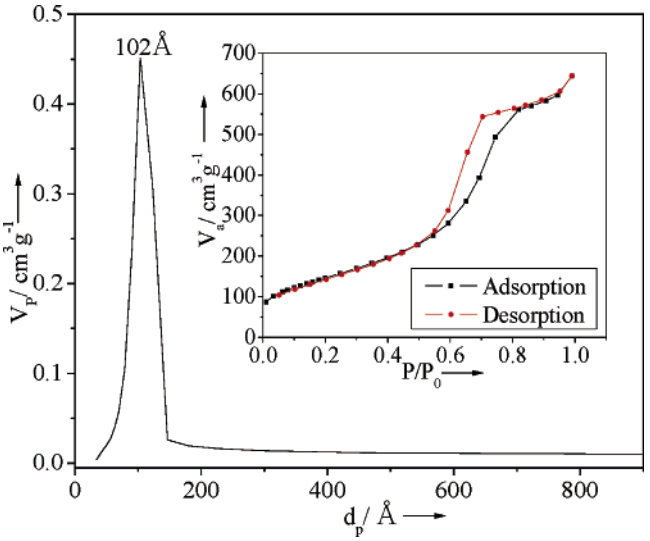

Figure 4. Nitrogen adsorption−desorption isotherm (inset) and the corresponding pore size distribution curve for calcined HLJU-10. V_a = volume absorbed; P/P_0 = relative pressure; V_p = pore volume; d_p = pore diameter. Nitrogen adsorption isotherms were obtained on a Micromeritics ASAP 2010 nitrogen adsorption apparatus. The Brunauer−Emmett−Teller (BET) equation was used to calculate the surface area from the adsorption branch. The pore size distributions were calculated by analyzing the adsorption branch of the nitrogen sorption isotherm using the Barret−Joyner−Halenda (BJH) method.

has large channel-like mesopores and a high degree of pore size uniformity. This is also substantiated by SEM, TEM, and the evolving pore size distribution plot. The calcined mesoporous HLJU-10 has a narrow BJH pore-size distribution with a mean

TABLE 1: Textural and Structural Parameters of Calcined Large-Pore Meso-nc-TiO_2 Samples with Different Pore Size Prepared Using P123 (1 g) as Template and Different Amount of Ti(OBu^n)$_4$ as the Titanium Source

Ti(OBu^n)$_4$ (g)	D_{pore}[a] (nm)	S_{BET}[b] ($m^2\,g^{-1}$)	V_t[c] ($cm^3\,g^{-1}$)	phase
2.6	8.3	151	0.328	anatase
2.7	10.2	134	0.237	anatase
3.0	12.1	121	0.221	anatase
3.4	14.0	115	0.219	anatase

[a] The average pore diameter is estimated using the adsorption branch of the isotherm and BJH model. [b] The specific surface area was calculated by BET method. [c] The total pore volume is taken from the the adsorption branch of the nitrogen isotherm curve.

value of 10.2 nm, a BET surface area of 134 $m^2\,g^{-1}$, and a pore volume of 0.237 $cm^3\,g^{-1}$.

It is noteworthy that tunable pore diameters in the range 8.3−14.0 nm can be reproducibly synthesized by altering the amount of Ti(OBu^n)$_4$ while other synthesis parameters are kept constant. The textural and structural parameters of the obtained calcined samples are summarized in Table 1. An observed trend is the increase of the mesopore size as the quantity of Ti(OBu^n)$_4$ is increased. This can be attributed to the following consideration: (1) The increase of Ti(OBu^n)$_4$ is paralleled by an increase in the amount of *n*-butanol released in situ. Pore size expansion upon increasing the amount of cosurfactant (BuOH or other *n*-alkyl alcohol) could be explained by the swelling in the hydrophobic to hydrophilic volume ratio of the block copolymer micelles.[6] The increase in the poly(propylene oxide) (PPO) core exceeds the increase in the poly(ethylene oxide) (PEO) corona (Figure 5).[17,20] With increasing Ti(OBu^n)$_4$, this effect becomes

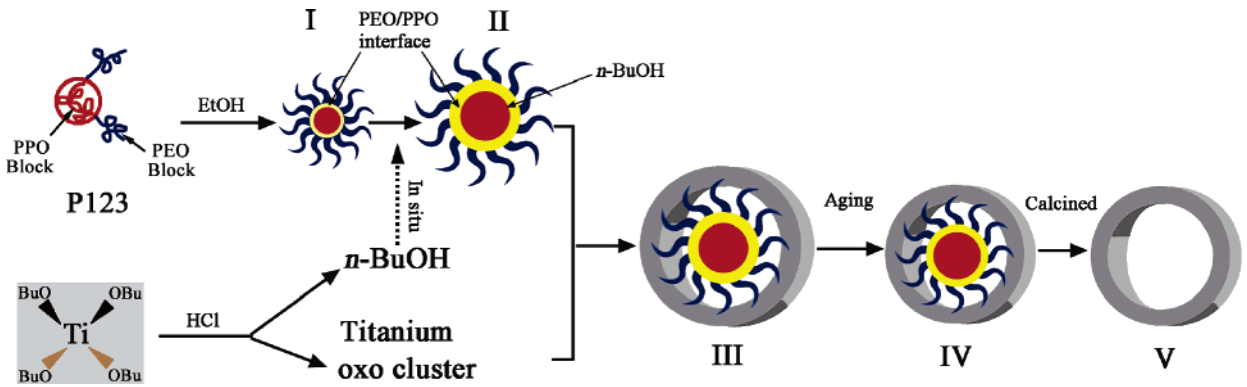

Figure 5. Schematic representation of the formation mechanism of the large-pore meso-nc-TiO_2 films presented in our proposed synthesis strategy. I: original block copolymer micelle. II: micelle swelled by *n*-BuOH released in situ. III: surfactant−titanium nanocluster complex. IV: well-defined and stable mesostructured hybrid. V: meso-nc-TiO_2 with large pore diameter.

more pronounced, and the PEO groups become more hydrophobic, resulting in wider pores. (2) The reactivity and spatial configuration of $Ti(OBu^n)_4$ derived from their linearities and dimensions should be taken into account. The hydrolysis−condensation of $Ti(OBu^n)_4$ produces Ti(IV) nanoclusters;[22] in the presence of triblock copolymer surfactant (P123, in our case), these species can in turn interact with the surfactant and thus modulate the hybrid interface. With the increase of $Ti(OBu^n)_4$, owing to the molar ratio of Ti/OBu = $^1/_4$, this effect becomes more prominent and results in larger mesopores with smaller pore volume and thus porosity.

4. Conclusion

In summary, we demonstrated a novel and facile synthesis strategy for the preparation of large-pore meso-nc-TiO_2 thin films using $Ti(OBu^n)_4$ as the inorganic precursor. The introduction of butanol in situ and the nature of the alkoxide groups result in the formation of uniform large mesopores. Moreover, the present large-pore meso-nc-TiO_2 thin films with tunable pore diameters in a narrow distribution of sizes ranging from 8.3 to 14.0 nm offer vast prospects for further applications in catalytic, adsorptive, and photovoltaic fields.

Acknowledgment. This work was supported by the Key Program Projects of National Natural Science Foundation of China (no. 20431030), the National Natural Science Foundation of China (no. 20301006), and program for new century excellent talents in university (NCET).

References and Notes

(1) Corma, A. *Chem. Rev.* **1997**, *97*, 2373−2419.

(2) Melosh, N. A.; Davidson, P.; Chmelka, B. F. *J. Am. Chem. Soc.* **2000**, *122*, 823−829.

(3) Göltner, C. G.; Henke, S.; Weissenberger, M. C.; Antonietti, M. *Angew. Chem., Int. Ed.* **1998**, *37*, 613−616.

(4) Yang, H.; Coombs, N.; Ozin, G. A. *Nature (London)* **1997**, *386*, 692−695.

(5) Liu, X.; Tian, B.; Yu, C.; Gao, F.; Xie, S.; Tu, B.; Che, R.; Peng, L.; Zhao, D. *Angew. Chem., Int. Ed.* **2002**, *41*, 3876−3878.

(6) Kim, T.-W.; Kleitz, F.; Paul, B.; Ryoo, R. *J. Am. Chem. Soc.* **2005**, *127*, 7601−7610.

(7) Kleitz, F.; Choi, S. H.; Ryoo, R. *Chem. Commun.* **2003**, 2136−2137.

(8) Kleitz, F.; Solovyov, L. A.; Anilkumar, G. M.; Choi, S. H.; Ryoo, R. *Chem. Commun.* **2004**, 1536−1537.

(9) Coakley, K. M.; McGehee, M. D. *Chem. Mater.* **2004**, *16*, 4533−4542.

(10) Smarsly, B.; Grosso, D.; Brezesinski, T.; Pinna, N.; Boissière, C.; Antonietti, M.; Sanchez, C. *Chem. Mater.* **2004**, *16*, 2948−2952.

(11) Crepaldi, E.; Soler-Illia, G. J. A. A.; Sanchez, C. *J. Am. Chem. Soc.* **2003**, *125*, 9770−9786.

(12) Crepaldi, E.; Soler-Illia, G. J. A. A.; Grosso, D.; Sanchez, C. *New J. Chem.* **2003**, *27*, 9−13.

(13) Soler-Illia, G. J. A. A.; Louis, A.; Sanchez, C. *Chem. Mater.* **2002**, *14*, 750−759.

(14) Yang, P.; Zhao, D.; Margolese, D. I.; Chmelka, B. F.; Stucky, G. D. *Nature (London)* **1998**, *396*, 152−155.

(15) Choi, S.; Mamak, M.; Coombs, N.; Ozin, G. *Adv. Funct. Mater.* **2004**, *14*, 335−344.

(16) Holmqvist, P.; Alexandridis, P.; Lindman, B. *J. Phys. Chem. B* **1998**, *102*, 1149−1158.

(17) Feng, P.; Bu, X.; Pine, D. *Langmuir* **2000**, *16*, 5304−5310.

(18) Holmqvist, P.; Alexandridis, P.; Lindman, B. *Macromolecules* **1997**, *30*, 6788−6797.

(19) Holmqvist, P.; Alexandridis, P.; Lindman, B. *Langmuir* **1997**, *13*, 2471−2479.

(20) Kleitz, F.; Blanchard, J.; Ågren, P.; Zibrowius, B.; Schüth, F.; Lindén, M. *Langmuir* **2002**, *18*, 4963−4971.

(21) Calleja, G.; Serrano, D. P.; Sanz, R.; Pizarro, P.; García, A. *Ind. Eng. Chem. Res.* **2004**, *43*, 2485−2492.

(22) Soler-Illia, G. J. A. A.; Sanchez, C. *New J. Chem.* **2000**, *24*, 493−499.